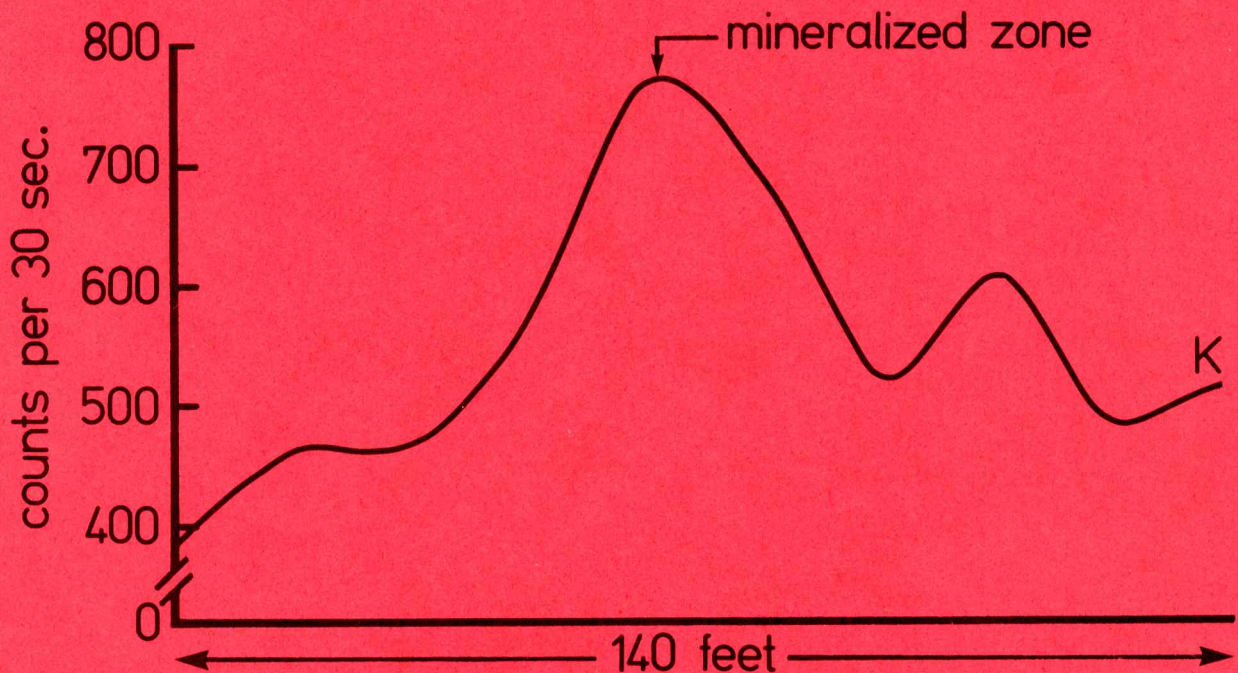


Exploration for Porphyry Copper Deposits through Multivariate Analysis of Computer-Registered Landsat and Geophysical Data Sets

by D.M. L'Heureux, D.W. Levandowski,
and P.E. Anuta



EXPLORATION FOR PORPHYRY COPPER DEPOSITS
THROUGH MULTIVARIATE ANALYSIS
OF COMPUTER-REGISTERED LANDSAT
AND GEOPHYSICAL DATA SETS

By

David M. L'Heureux
Graduate Student, Department of Geosciences
Purdue University

Don W. Levandowski
Professor, Department of Geosciences
Purdue University

Paul E. Anuta
Associate Program Leader
Laboratory for Applications of Remote Sensing
Purdue University

This work was sponsored by the National Science Foundation
under Grant ENG7820466

ABSTRACT

Aeroradiometric and Landsat reflectance data collected over an area in southeastern Arizona were computer-registered and subjected to multivariate analysis as a means of exploring for porphyry copper deposits. Based on a knowledge of the geological and geophysical characteristics of these deposits, an exploration variable, $P = K + K/Th + MSS\ 5/MSS\ 4 + MSS\ 6/MSS\ 7 + U + U/Th$, was formed and employed to target areas of mineralization potential. Of the five anomalies targeted and field-checked, three proved to be of exploration interest. Two of these anomalies were caused by hydrothermally-altered fault zones while the third appeared related to altered rock detritus on a mountain pediment. The technique should prove very useful in reconnaissance exploration of new areas.

INTRODUCTION

The value of integrating remotely-sensed data from satellites into the exploration process has been demonstrated over the past several years (see review article by Simpson, 1978). The present trend towards automating the concurrent analysis of satellite and other data types can also aid the exploration effort, as this method provides a means by which these various data can be specially combined and then applied to a particular exploration problem in an expeditious manner.

Computer-oriented integration techniques permit various data types to be registered to a common grid and operated on simultaneously. The data can be manipulated on a cell-by-cell basis in such a way as to rapidly educe a particular pattern of interest. In mineral exploration, this pattern would be the collective expression of the geological and geophysical characteristics of a specific type of mineral deposit. The particular data types employed in an exploration effort are those which concertedly can detect this collective expression or "signature." The specific manipulation of the data types that is necessary in order to rapidly detect the signature is dictated by the exploration model being followed. This approach guarantees that the sites targeted for exploration within a study area have the greatest potential for mineralization.

APPLICATION TO PORPHYRY COPPER EXPLORATION

One type of mineral deposit amenable to this exploration technique is the porphyry copper deposit. These deposits possess a number of features, listed in Table 1, whose characteristic expressions are detectable by two current remote sensors: the Landsat multispectral scanner and the airborne gamma-ray ($\text{Bi}^{214}(\text{U})$, $\text{Tl}^{208}(\text{Th})$, K^{40}) spectrometer. These features can thus be incorporated into a multivariate exploration model.

The first feature of interest, hydrothermal alteration, results from the activity of hydrothermal solutions in and near the hot copper-bearing intrusive. These solutions introduce considerable amounts of potassium into the host and adjacent country rocks through the formation of such alteration minerals as orthoclase, biotite, and sericite (Lowell and Guilbert, 1970). This increase in potassium content is detectable by a gamma-ray spectrometer tuned to the energy peak of the radioactive isotope, K^{40} . Davis and Guilbert (1973) demonstrated by ground surveys at a number of open-pit copper mines in Arizona that a strong increase in potassium radioactivity occurs towards the centers of the deposits. Such a phenomenon should be detectable with a low-altitude airborne gamma-ray survey as well. In addition, high values of the radioelement ratio, K/Th , should also be observed over a deposit as thorium is not preferentially localized through hydrothermal alteration (Davis and Guilbert, 1973; Moxham et al, 1965). Both "high K" and "high K/Th " are thus components of the detectable porphyry copper signature.

Table 1. Features and Resulting Signature of
Porphyry Copper Deposits

<u>Feature</u>	<u>Expression</u>
Hydrothermal Alteration	High K, K/Th
Oxidation of Sulfides (especially pyrite)	High $\frac{MSS5}{MSS4}$, $\frac{MSS6}{MSS7}$
Possible Uranium Enrichment	High U, U/Th

The second feature of interest is the oxidation of sulfides that occurs in the near-surface zone of these deposits. It is the oxidation of the ubiquitous sulfide mineral, pyrite, that is primarily responsible for the iron oxide gossans (principally hematite and goethite) which cap porphyry copper deposits (Schwartz, 1966). Numerous studies over the past several years have demonstrated that Landsat ratios MSS 5/MSS 4 and MSS 6/MSS 7 are capable of detecting outcrops with high iron oxide content (Vincent, 1973; Salmon and Vincent, 1974; Lyon, 1977; Kowalik et al, 1980). This capability is due to the fact that iron oxide minerals have iron absorption bands in their spectra which reduce their reflectance in the bandwidths that are sensed by Landsat bands 4 and 7 (c.f. Hunt and Ashley, 1979) and this results in anomalously high values of MSS 5/MSS 4 and MSS 6/MSS 7 over limonitic exposures. Both "high MSS 5/MSS 4" and "high MSS 6/MSS 7" are thus two more components of the detectable porphyry copper signature.

The final feature of interest is the possible uranium enrichment associated with these deposits. Although not a characteristic of porphyry coppers, uranium minerals (commonly tobernite) have been found in the oxidized zone of many deposits (Moxham et al, 1965; Lynch, 1966; Moolick and Durek, 1966) and appear to be often associated with the porphyry copper-molybdenite deposits (Brown and Cathro, 1976). Naturally, any increase

in uranium radioactivity above normal background would be detectable with an airborne gamma-ray spectrometer. In addition, high values of the radioelement ratio, U/Th, should also be observed over a deposit if there is an increase in uranium content. Both "high U" and "high U/Th" comprise the final components of the detectable porphyry copper signature.

The exploration model for porphyry copper deposits should be designed so as to detect the porphyry copper signature in a rapid and efficient manner. Since the signature as described above is comprised of high values of each of six variables, the logical approach would be to add these variables to produce a new variable whose very highest values could then be used to target areas of greatest mineralization potential. This new variable, $P = K + K/Th + MSS\ 5/MSS\ 4 + MSS\ 6/MSS\ 7 + U + U/Th$, would thus serve as a means of enhancing common anomalies over normal background. Any area exhibiting anomalously high values of a majority of the six variables would produce a very high value of the variable P and thus would be a prime candidate for field examination. This model is very efficient as it compresses the information of six variables into one variable, and thus offers a considerable savings in time and expense. It is also rapid to implement once the data are in a registered format. Furthermore, the model is very simple as it requires no a priori knowledge of the actual ranges of values of the multivariate signature.

To test the utility of computer-registered data sets in general and the porphyry copper exploration model in particular,

this technique was applied to a study area within the porphyry copper province of southeast Arizona.

THE STUDY AREA

The study area lies southwest of Tucson and covers approximately 1,330 sq. mi. (Fig. 1). It includes the Sierrita Mountains and surrounding pediment to the north, is terminated to the south by the U.S.-Mexican border, and is bracketed on the east and west by the Santa Rita and Baboquivari Mountains, respectively. The dominant rock unit as mapped is Quaternary alluvium, followed in order of decreasing abundance by Tertiary plutonic and volcanic rocks, Mesozoic volcanic and plutonic rocks, and sedimentary rocks of varied age (Arizona Bureau of Mines, 1969).

This particular area was chosen for study because (1) aeroradiometric and Landsat data of good quality were available for the area, and (2) it contains extensive stretches of mountain pediment, presently a major focus of porphyry copper exploration. Indeed, four open-pit copper mines are located on the eastern pediment of the Sierrita Mountains just within the northeast corner of the study area. These mines, along with two other mines located within the Sierrita Mountains proper, provide 25% of the nation's copper production (U.S. Bureau of Mines, 1977).

DATA ACQUISITION AND REGISTRATION

Aeroradiometric data (U,Th,K) collected as part of the National Uranium Resource Evaluation (NURE) program were obtained for the study area as were Landsat computer compatible tapes. The aeroradiometric data were collected at a nominal altitude of 400 feet along north-south flightlines that were spaced approximately three miles apart. The along-track sample spacing was 450 feet. Data reductions included an onboard background radiation correction, cosmic and atmospheric radiation corrections, and normalization to a constant 400-foot vertical terrain clearance. However, no data collected above an altitude of 700 feet were used in this study. The Landsat data were collected on February 8, 1975 under a solar elevation angle of 31° . The data underwent standard geometric corrections, but were not radiometrically corrected as this study was not concerned with absolute reflectances.

These two data sets were integrated using an in-house computer-registration technique (Anuta, 1977). The registration is based on a uniform grid system which divides a study area into resolution cells that are 500 feet square. Each data set is registered to this grid using a nearest-neighbor rule (Fig.2). The aeroradiometric data in this study were easily registered as every third data record had associated with it a latitude/longitude coordinate. Records falling between these controlled locations were registered by interpolation. The Landsat data were initially rubbersheet matched to the grid through control

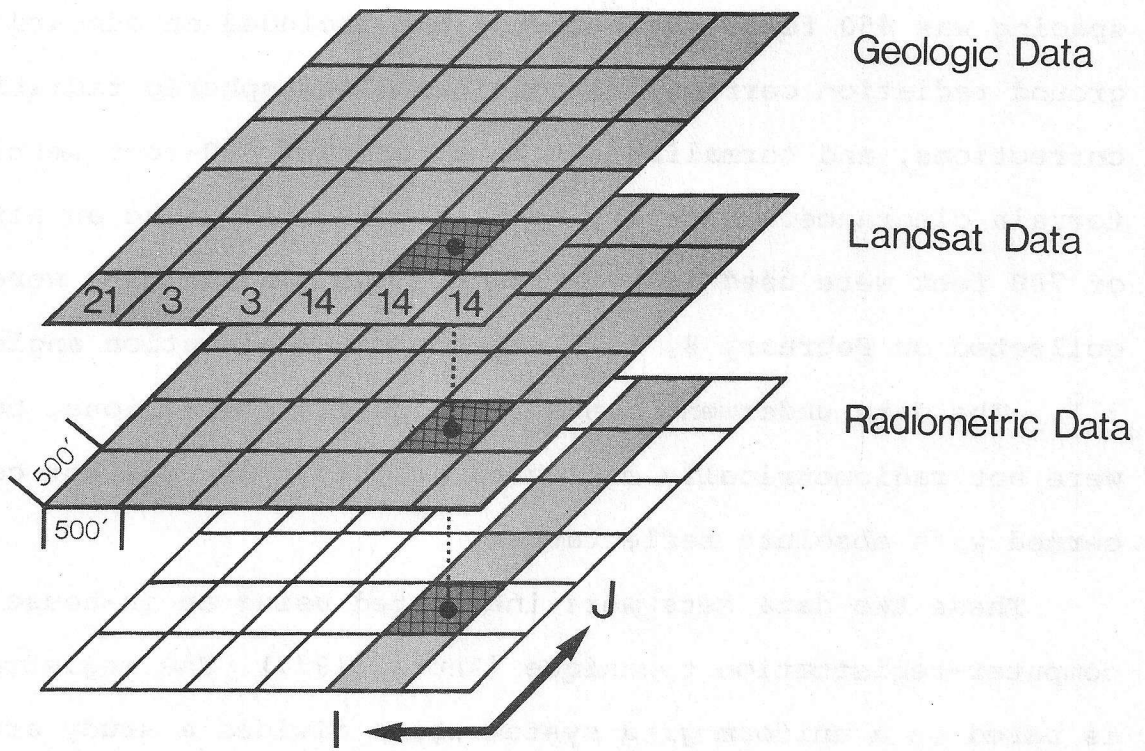


Figure 2. Illustration of multivariable registration. Resolution cells are addressable by one coordinate pair and a channel pointer.

point registration before nearest-neighbor allocation. The computer-registration technique permitted a maximum possible registration error of 353 feet for the radiometric data, and an rms error of 1.5 pixels for the Landsat data. As the radiometric data were constrained to the aircraft flightlines, only those resolution cells which fell along the flightlines were used in this study.

In addition to the aeroradiometric and Landsat data, geologic data were also registered to this grid. This was done in order to permit analysis on a "per rock type" basis. The data were obtained by digitizing a 1:250,000 scale geologic map of the study area. Each rock type was assigned a number to uniquely identify it and these numbers were loaded directly into the grid (Fig. 2). The maximum error in the geology registration was about .6 resolution cells or 300 feet. A computer-plotted display of the geology data set is shown in Figure 3a. A photo of the study area from the state geologic map is shown in Figure 3b for visual comparison.

DATA PREPARATION

The registered data sets were stored on magnetic tape in order to undergo computer-oriented multivariate analysis. After producing the ratios K/Th , U/Th , $MSS\ 5/MSS\ 4$, and $MSS\ 6/MSS\ 7$, each variable (including U and K) was linearly scaled so as to fill the available dynamic range of the byte-oriented system (0-255). This type of scaling had the effect of increasing the

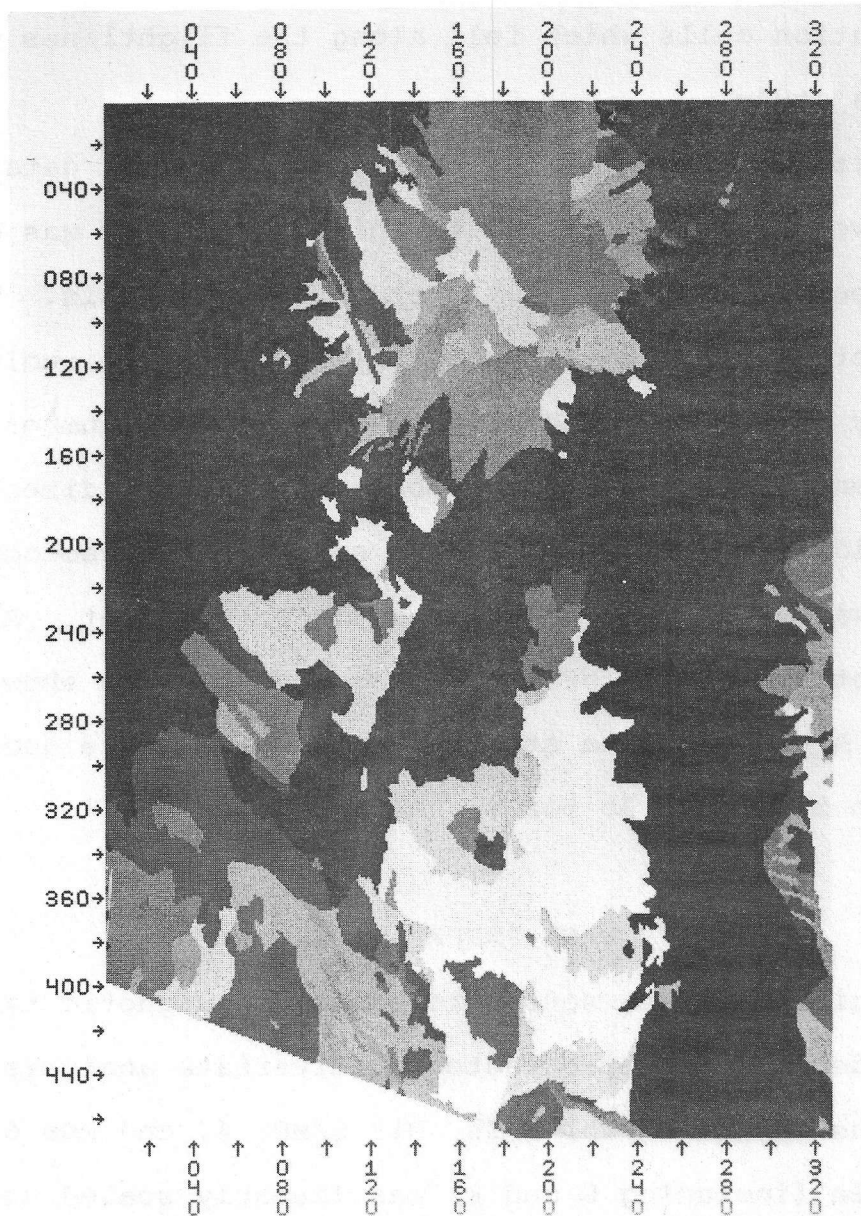


Figure 3a. Computer-plotted display
of the Geology Data Set.

separation between the higher and lower values of the distributions; a condition which militated toward improving the discriminating power of the exploration variable P. Later analysis showed that the unequal standard deviations of the variables did not cause a significant bias in the variable P. After scaling, the variables were added to produce P, which itself was then scaled to 0-255.

A histogram of the variable P was subsequently produced for the 4,123 resolution cells comprising the data set (Fig. 4). Because the histogram was Gaussian in form, it was decided that the anomaly threshold level should be set at +2 standard deviations, thereby restricting the anomaly classification to a small percentage of the population. All values of the variable P which were greater than +2 standard deviations from the mean were considered anomalous and therefore of interest in the search for porphyry copper deposits. One hundred and forty-four data values fell into this category and these were computer-plotted at a scale of 1:250,000 to produce the anomaly map (Fig.5).

The selection of the anomalous data values was based upon a histogram which involved data collected over 24 different rock types. In order to determine whether any data values were excluded from being classified as anomalous because of the use of a group threshold level, a histogram of the variable P was produced for each individual rock type. Out of the 13 rock types for which a standard deviation could be calculated (>20 data

$$P = K + K/Th + \frac{MSS5}{MSS4} + \frac{MSS6}{MSS7} + U + U/Th$$

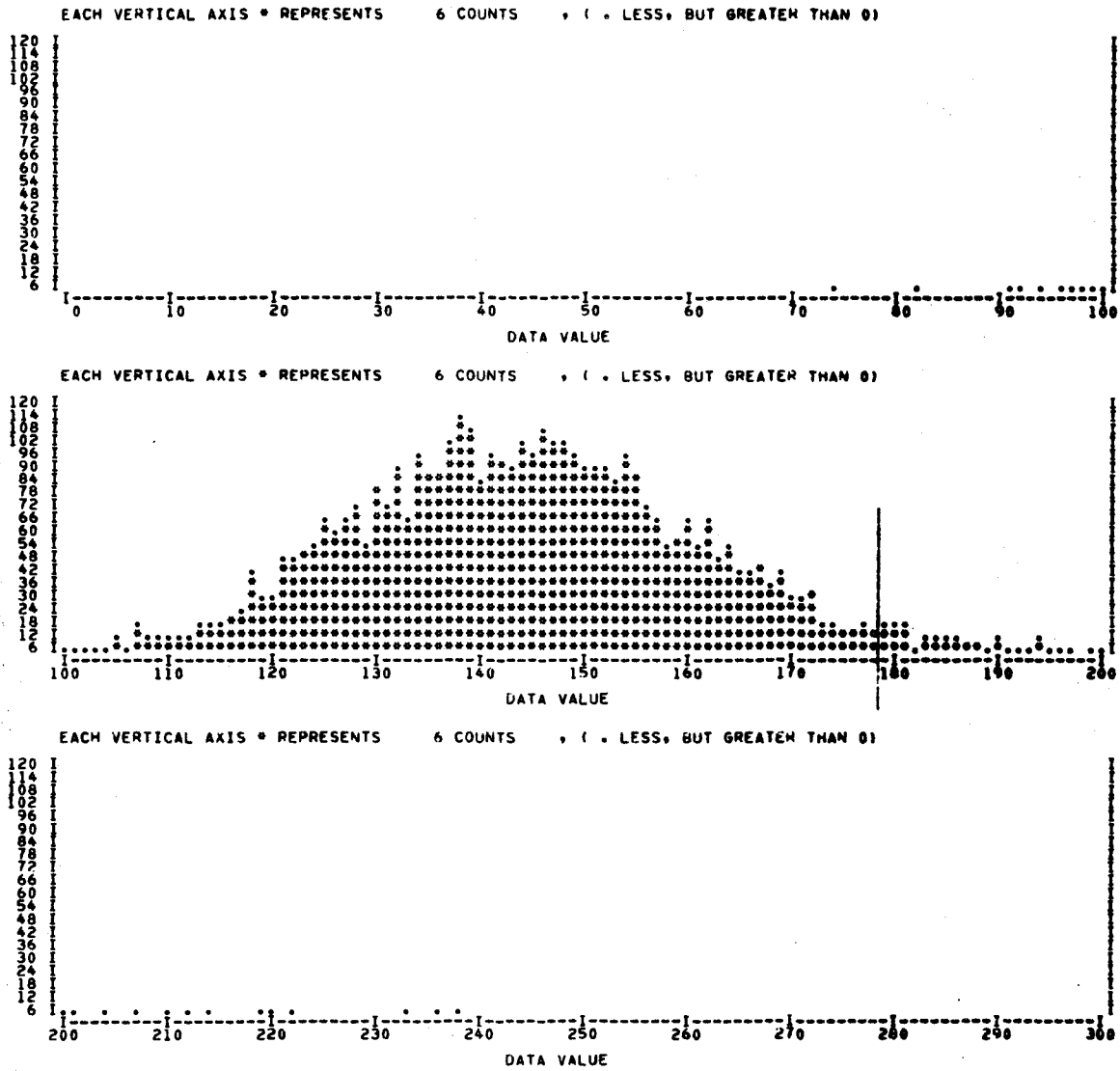


Figure 4. Histogram of the variable P for the 4,123 resolution cells in the data set. Vertical line marks the +2 standard deviation threshold.

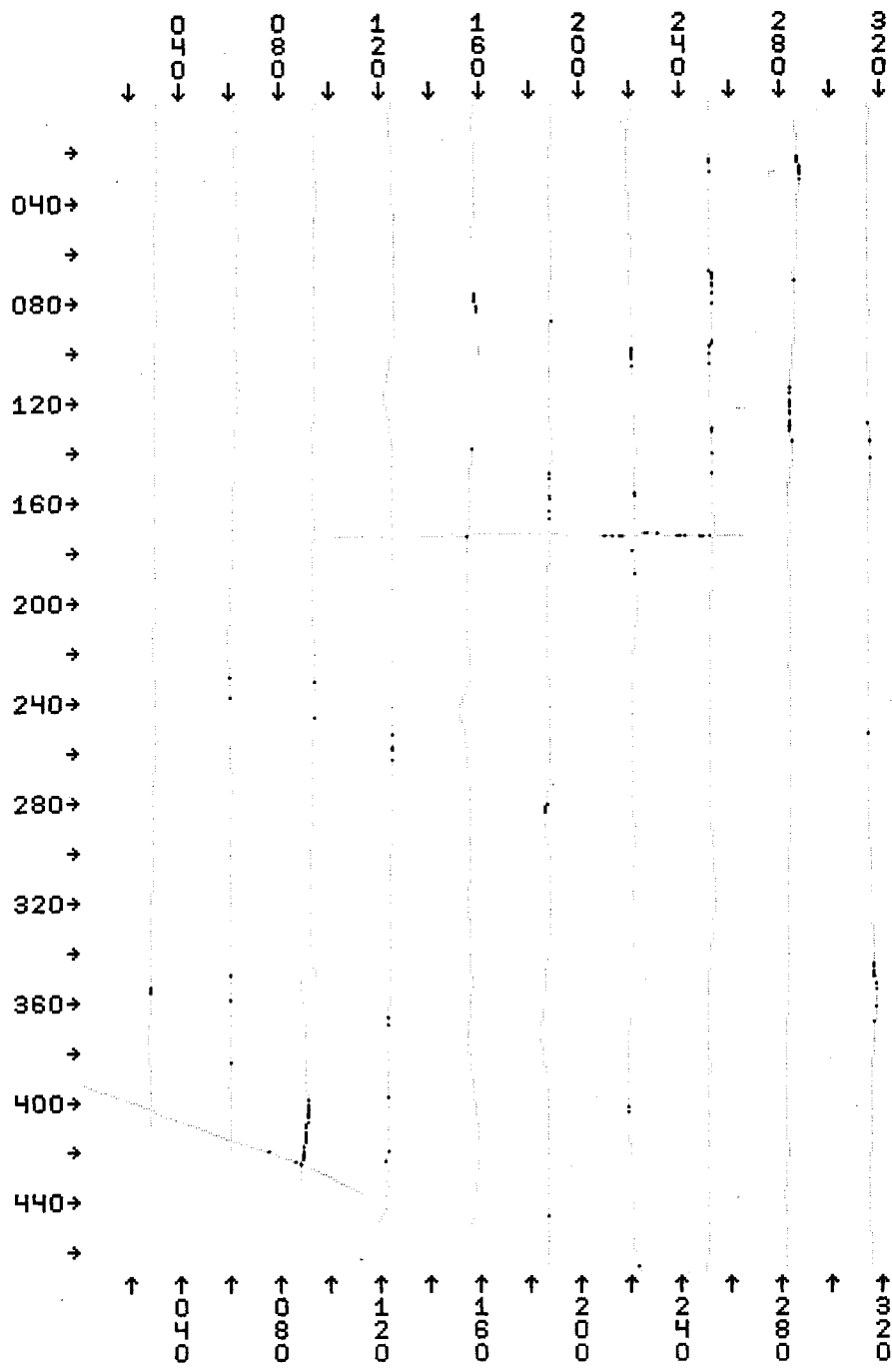


Figure 5. Anomaly map of the study area. The black squares indicate the anomalous points while the dotted lines indicate the aircraft flightlines. Compare with Fig. 1.

points), three had anomalous data values ($\geq + 2$ standard deviations) which fell below the group threshold level. These few additional anomalous data values were included along with the original set for analysis.

DATA ANALYSIS

The initial phase of analysis involved examining the anomalous points to determine whether any had an obvious source and thus could be removed from further consideration. This was the case for most of the points in the northeast section of the anomaly map. These points are located over the open-pit copper mines and mine dumps of the Pima mining district. Other points removed from further consideration were those which clearly followed the outcrop exposure of a particular rock unit. This was the case for the Josephine Canyon quartz monzonite which is situated along the southeast margin of the study area. The anomalous points clearly mark the outcrop exposure of this inherently radioactive rock for a distance of $1\frac{1}{2}$ miles. Further points disregarded were those that were anomalous only because they exhibited exceedingly low values of thorium radioactivity. Very low thorium counts will produce U/Th and K/Th ratio values that are very high and thus result in anomalous P values even though the U and K counts themselves are only average. This was the case for the points located over Cretaceous andesite in the west-central section of the study area. Finally, a number of points were disregarded because they appeared to be due entirely

to favorable source-detector geometry, such as would occur when flying over a narrow V-shaped valley. In all, 79 anomalous points survived this initial screening process and these were passed on for further study.

The locations of these remaining anomalous points were carefully examined on aerial photographs in order to determine whether any circular or linear features were present in the area. In addition, aeromagnetic data from these locations were also examined so as to detect any change in magnetic intensity. The aeromagnetic data had been obtained along with the aeroradiometric data from the NURE survey and were used in this study as a separate source of information. From these final analyses emerged five anomalies (comprising 33 anomalous points) that were considered to be worthy of field examination (Fig. 6). Of the 5, only 3 proved to be of exploration interest.

DISCUSSION OF THE ANOMALIES

Anomalies 1 and 2

The first anomaly was of interest mainly because it exhibited extremely high values of potassium radioactivity (≥ 2 s.d.) and was situated over an interesting circular feature. The anomaly was further characterized by only average values of the U, MSS 5/MSS 4 and MSS 6/MSS 7, but very high values of K/Th and U/Th (≥ 1.5 s.d.) due in part to somewhat low counts of Th. In the field, the anomaly proved not to be due to an intrusive but to an exposure of high potassium-bearing

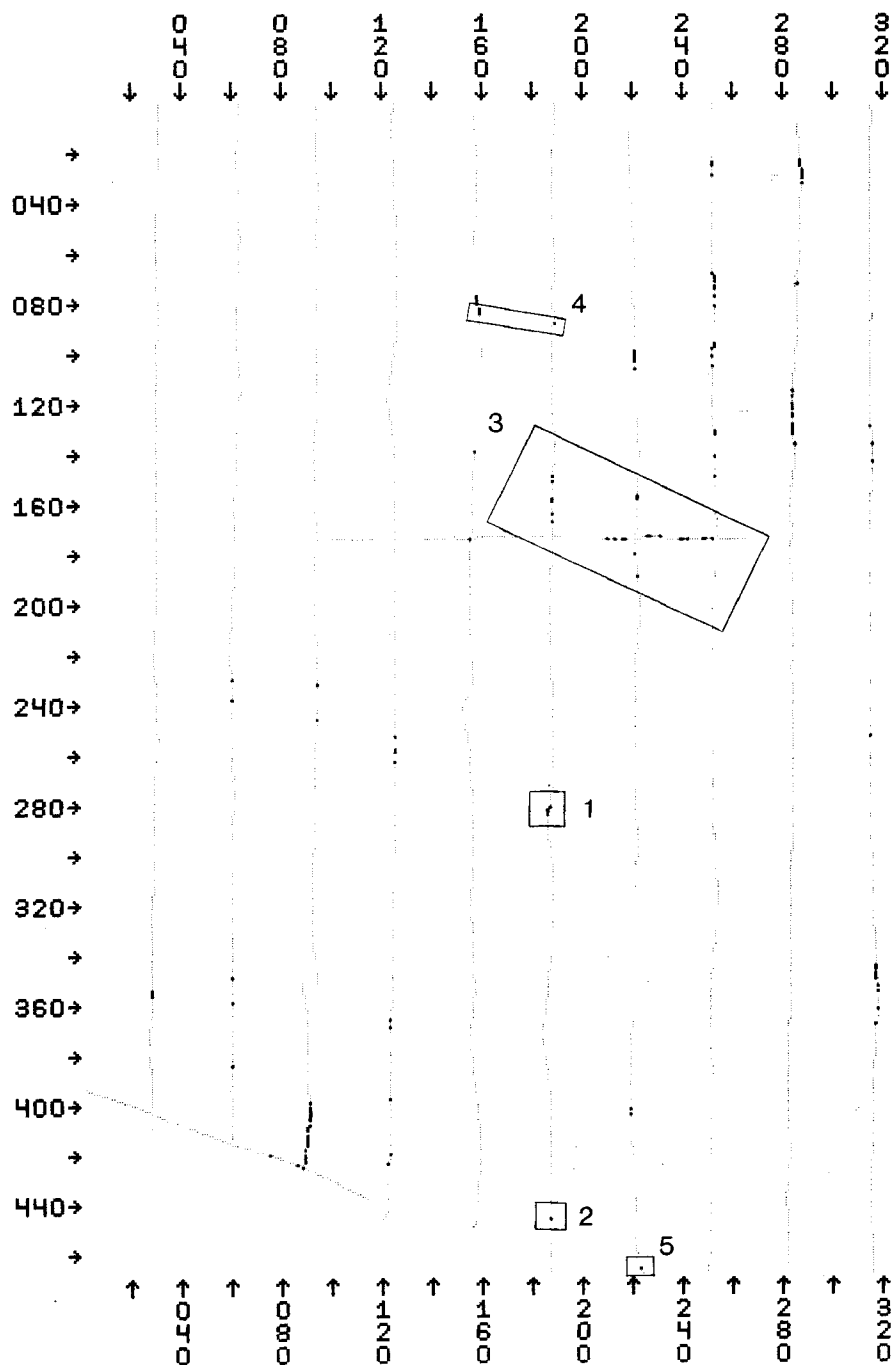


Figure 6. Anomaly map showing the locations of the five anomalies that were field-checked.

epiclastic rocks. The circular feature was found to be erosional in nature and not fault-controlled. The anomaly was therefore nonsignificant and will not be discussed further.

The second anomaly was characterized by a very high value of U, high values of K and U/Th (≥ 1 s.d.), a fairly high value of K/Th (.5-1 s.d.), and average values of MSS 5/MSS 4 and MSS 6/MSS 7. It was also located at the intersection of two prominent linears. In the field, however, the anomaly was found to be due only to an exposure of Tertiary silicic volcanic rocks that were more inherently radioactive than were the nearby volcanic rocks of Cretaceous age. The anomaly was therefore considered nonsignificant and not of further interest here.

Anomaly 3

The third anomaly was of interest because it was located on the pediment of the Sierrita Mountains, an expanse that already has yielded a number of porphyry copper deposits. The anomalous points shown within rectangle number 3 in Figure 6 are characterized by average to high values of U, U/Th, MSS 5/MSS 4, and MSS 6/MSS 7; high values of K/Th, and very high values of K. Indeed, the shape of the anomaly is shown best by the potassium radioactivity data (Fig. 7). When transferred onto an aerial photograph, the anomaly definitely proves to be alluvium-derived (Fig. 8). What makes the anomaly interesting is the fact that very high potassium radioactivity is not detected on the pediment directly to the east of the nose

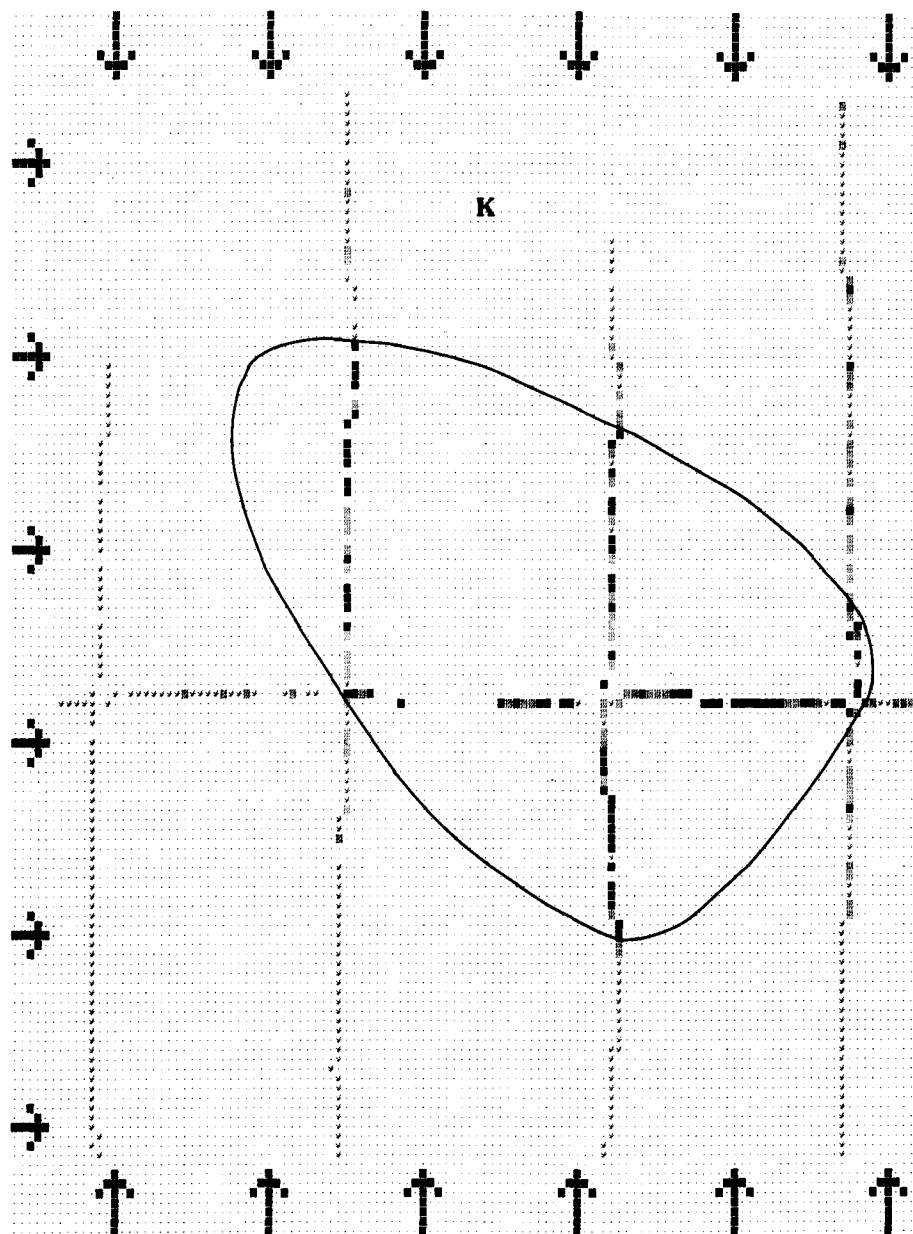


Figure 7. Computer-plotted display of the potassium radioactivity data for the area of Anomaly 3. The black squares indicate data values that are greater than +1.5 standard deviations from the mean of the potassium distribution; the grey squares indicate data values that lie between +1.5 and +1 standard deviations from the mean; and the V-shaped symbol indicates data values that fall below +1 standard deviation from the mean. The black ellipse outlines the area of the anomaly.

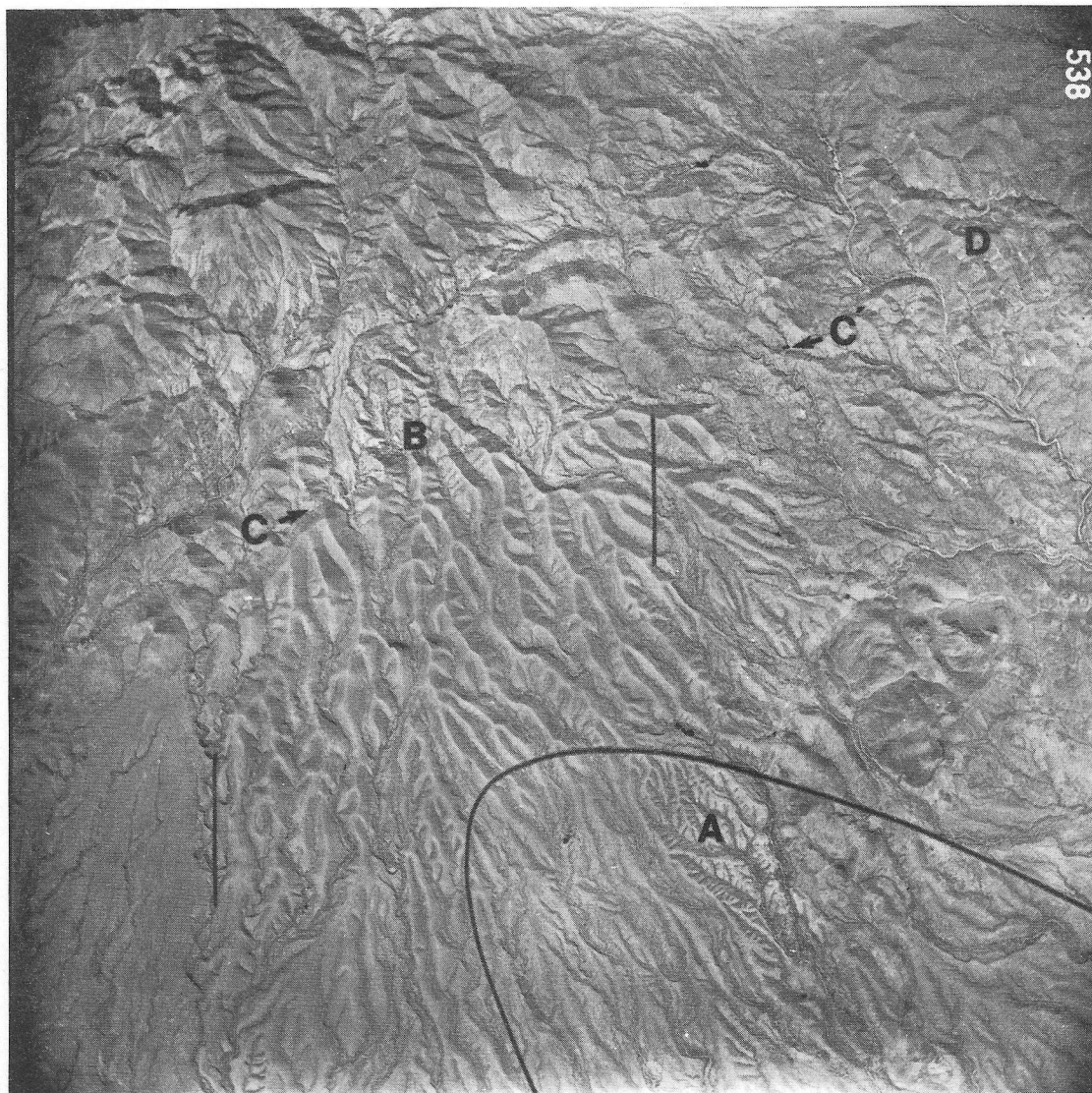


Figure 8. Aerial photograph taken in 1955 showing the location of Anomaly 3 on the southern pediment of the Sierrita Mountains. The two vertical bars indicate the positions of the aircraft flightlines and are one mile in length. See text for explanation of lettering.

of the anomaly nor directly to its north. This would be expected if the anomaly were due solely to the detritus of the rhyolitic rocks which make up much of the southern flank of the Sierrita Mountains (Cooper, 1973). A more localized source is apparently contributing to the anomaly.

In order to better understand the cause of the anomaly, a field examination was conducted at locality A in Figure 8. Although the subsurface formation in the area was Tertiary conglomerate with volcanic clasts, the weathered surface material appeared to comprise a large concentrate of plutonic rocks. Examination of numerous grab samples and the later study of thin sections showed this plutonic rubble to be highly altered. The most common rock type recognizable was fine-to-medium-grained quartz monzonite. Alteration features observed included veinlets composed of quartz and potassium feldspar; sericite and clay minerals after plagioclase; abundant secondary K-spar, K-mica, and quartz; and limonitic crusts after pyrite. The rocks were also iron-stained. Measurements made with a portable gamma-ray spectrometer further showed that this surface rubble was more radioactive from potassium-40 than was the underlying conglomerate. It is possible then, but hardly proven, that the anomaly on the southern pediment is due to this altered rock detritus. The radiation from the increased potassium content could very well be the cause of the high K/Th and very high K anomalies detected over this area. Since this type of altered rock is what one might expect to find near a weathered porphyry

copper deposit, it is of interest to try and locate the source area of this flood-borne detritus.

Examination of the drainage pattern in Figure 8 indicates that only locality B could serve as the source area for the elliptical anomaly and still not significantly affect the areas lying outside the ellipse. However, it is considered unlikely that a large exposure of altered quartz monzonite could escape attention in this well-explored region. Furthermore, the anomaly seems much too large to have been derived solely from an exposure within this small area. One plausible theory is that the source rock was indeed located at position B during early-middle Quaternary time, but has since been tectonically transported away. This theory is based on the presence of a major strike-slip fault (C-C' in Fig. 8) which separates the pediment from the highlands at locality B and also intersects the Esperanza porphyry copper deposit to the northeast (D in Fig. 8). The disparate terrains on either side of the fault plus its very "fresh" appearance make it feasible that recent strike-slip movement has occurred along it. The altered rock detritus which overlies the Miocene-Pliocene conglomerates of the southern pediment may very well have been derived from the quartz monzonite associated with the Esperanza porphyry copper deposit during early Quaternary time, before tectonic forces acted to transport the deposit northeastward to its present location. Detailed field examination of the fault zone should determine whether this scenario is tenable. If not, then further

attention should be devoted to unravelling the complex fault movements of the southern Sierritas in order to better determine the present whereabouts of the "missing" porphyry copper deposit.

Anomaly 4

The fourth anomaly actually comprises two anomalous locations in the central Sierrita Mountains (localities A and C in Fig. 9). The anomalous points, located on adjacent flightlines, are characterized by average values of MSS 5/MSS 4 and MSS 6/MSS 7; high values of U, U/Th, and K/Th; and very high values of K. The western anomalous points also exhibit an aeromagnetic low relative to the adjacent points to the north and south. The anomaly was of interest because it was coincident with the Sierrita fault zone, a major feature that is believed to have exerted structural control on the emplacement of the Sierrita porphyry copper deposit (Lootens, 1966).

In the field, high levels of radioactivity were measured with the portable gamma-ray spectrometer at locality A in Fig. 9. However, the erratic exposures made it difficult to determine the exact source of the radiation. It was only by following one of the main faults down strike to where it intersected a roadcut (locality B in Fig. 9) that the true source of the radiation became known. Here, altered and shattered andesitic rocks within a zone about 20 feet wide are in sharp contrast with unaltered massive andesites on either side. The altered rocks are markedly bleached on fresh surfaces while

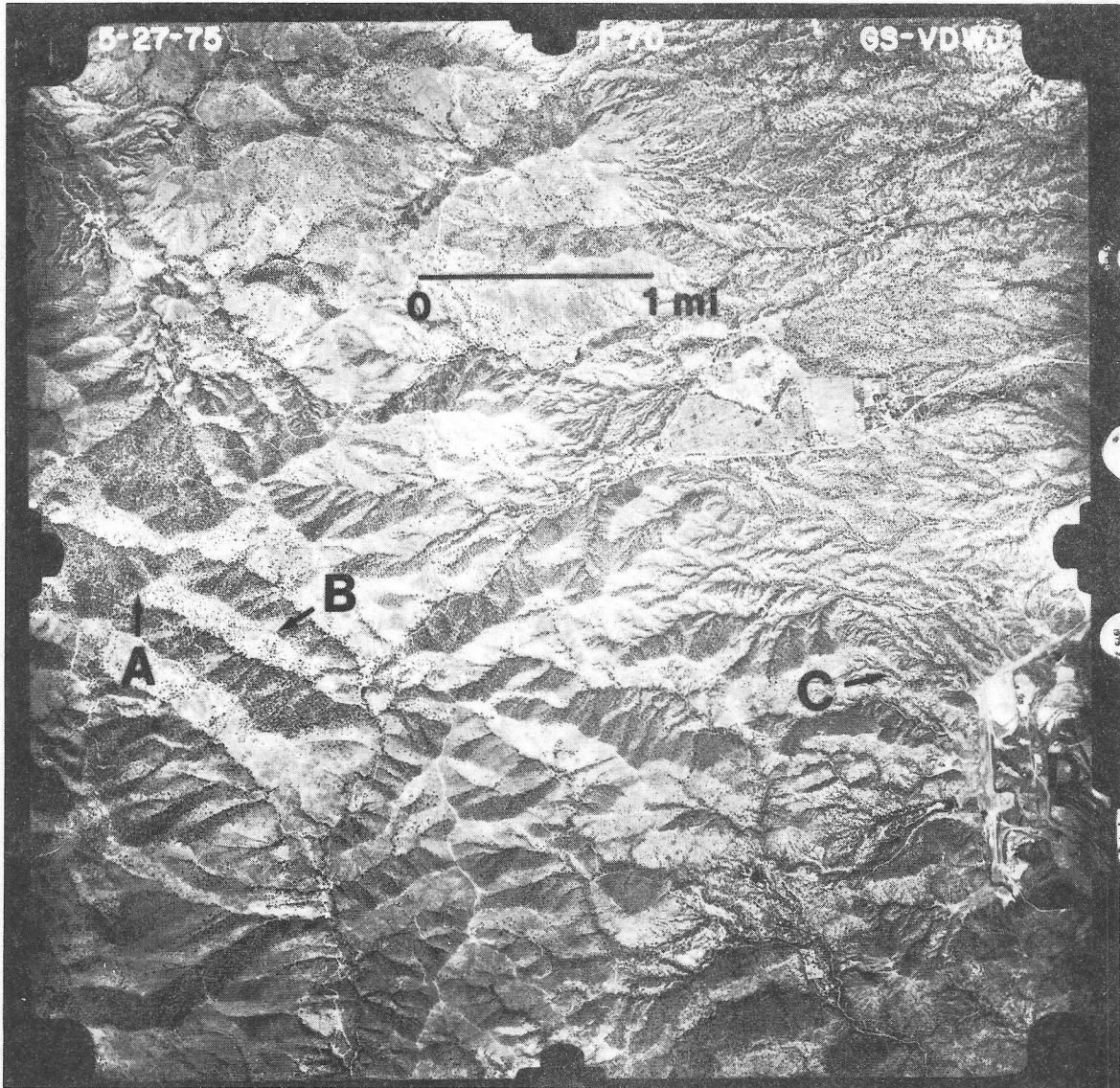


Figure 9. Aerial photograph showing the area of Anomaly 4 in the Sierrita Mountains. See text for explanation of the lettering.

their weathered surfaces are stained with iron oxides and an irridescent blue coloration that is possibly a copper sulfide alteration product. Pyrite is seen filling many of the smaller fractures in the central portion of the fault zone. Thin sections of the altered rock show it to be highly sericitized near veinlets of pyrite. A radiometric profile of the fault zone was made in order to determine if the sericitic alteration could be responsible for the very high potassium radioactivity levels measured by the aerial survey at locality A. As the graph in Figure 10 show, this indeed is probably the case. However, the graph does not show evidence of high uranium radioactivity as was measured at locality A.

The same visible signs of major faulting and alteration were also observed at the second anomalous locality (C in Fig 9). The strike of the altered gouge zones in this area continues the trend of the Sierrita fault zone. If extended, this trend would run almost tangent to the northern rim of the Sierrita open-pit mine (D in Fig. 9).

It therefore appears that the Sierrita fault zone, in addition to its role in controlling the emplacement of the Sierrita deposit, was also a major conduit in the hydrothermal convection system set up by the invading intrusive. The detection of such hydrothermally-altered fault zones in other mountainous areas would thus be a good indication of a possible nearby porphyry copper deposit.

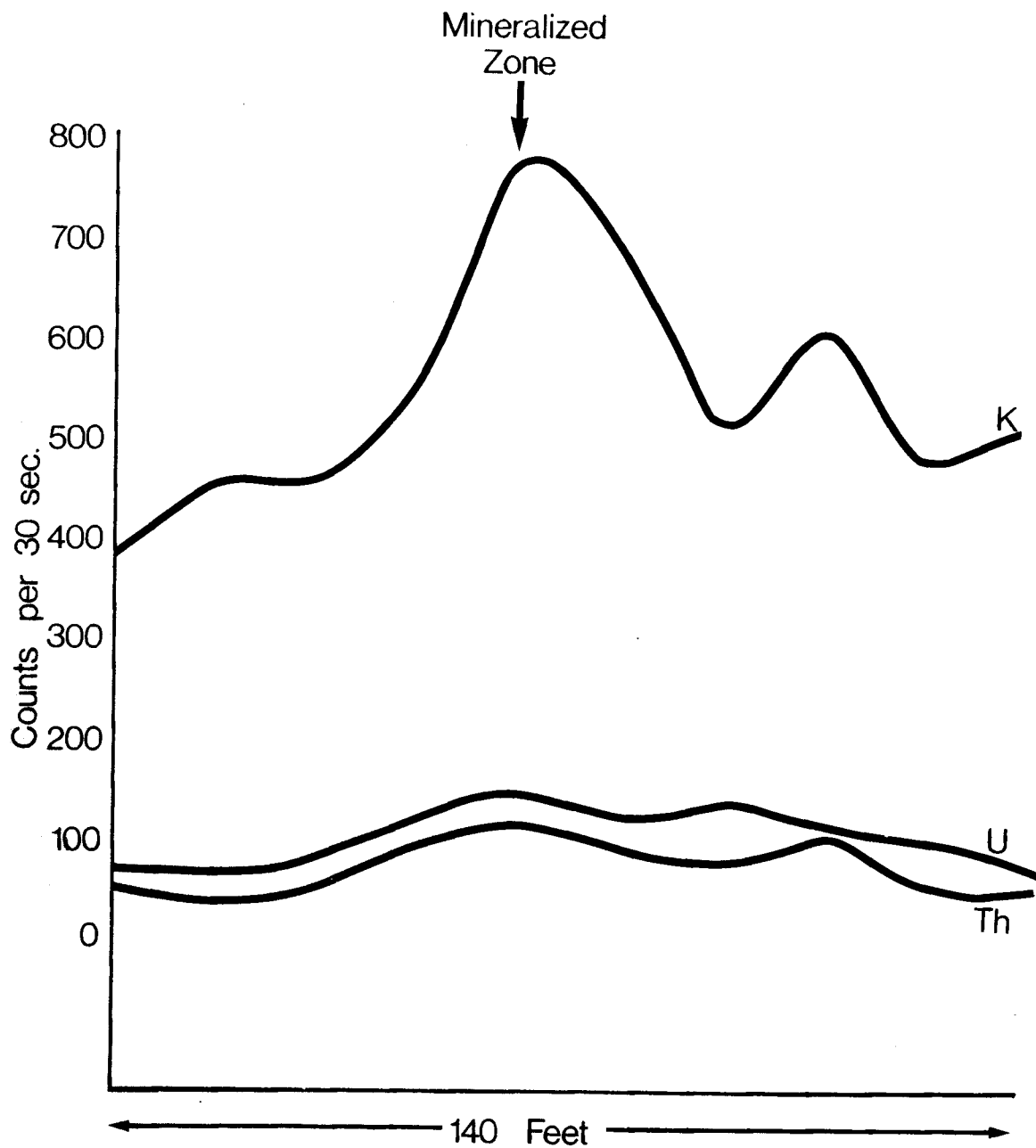


Figure 10. Radiometric profile of the wall rock taken along the roadcut at locality B in Fig. 9. The position of the hydrothermally-altered fault zone is as indicated.

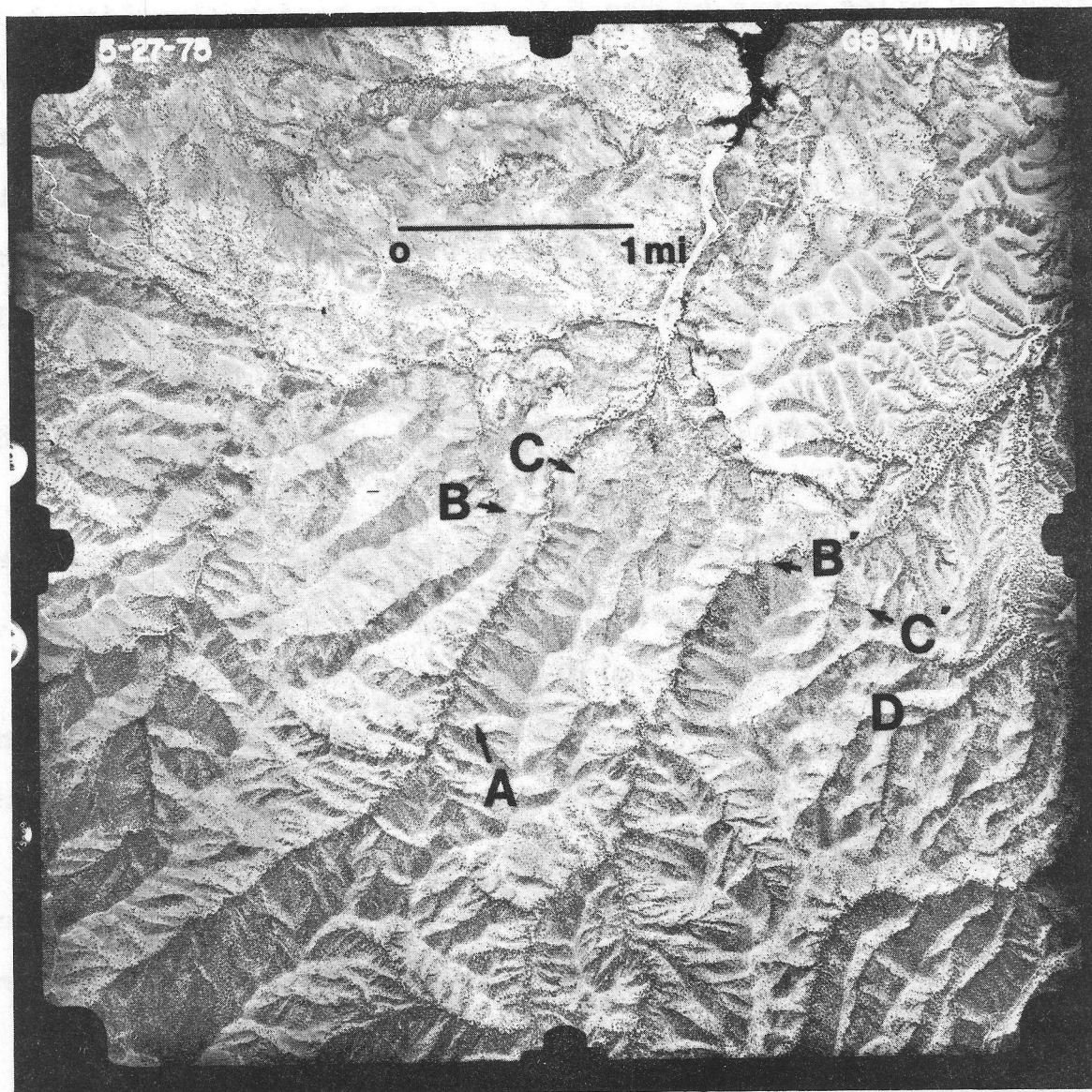


Figure 11. Aerial photograph showing the area of Anomaly 5 in the Pajarito Mountains. See text for explanation of lettering.

Anomaly 5

The fifth and final anomaly comprises one anomalous point and is located in Pena Blanca canyon in the Pajarito Mountains about 30 miles north of the U.S.-Mexican border (locality A in Figure 11). The point exhibits average values of U/Th and K/Th, a high value of U, and an extremely high value of K. The Landsat ratios provide no information as the area was in shadow at the time of data acquisition. The anomalous point also lies at the center of a narrow aeromagnetic low. The existence of a subtle linear feature seen extending through the anomaly under stereoscopic examination provided final impetus for the field examination.

In the field, the outward signs of a hydrothermally-altered fault zone were definitely in evidence along the canyon wall. Over a distance of less than 50 feet, the normally massive, pinkish rhyolite porphyry was highly crushed and displayed the same bleached tones, red and iridescent blue colorations, and sericitic alteration that had been observed in the altered fault zone in the Sierritas. Across the wash on the opposite slope face, the fault zone was easily discernible as it formed a notch in the hillcrest that was the apex of an apron of pulverized, yellow-brown talus. The brecciated rock in the fault zone most certainly contributed to the very high levels of radioactivity by offering more total surface area for radiation emission.

In addition to this fault zone, there are a few, more

prominent faults in the area to the northeast. Trending northwest-southeast, these faults are quite noticeable on large-scale aerial photographs. Two of them in particular are marked by small mines (B-B' and C-C' in Fig. 11). When extended to the southeast, these faults intersect the extension of the east-northeast-trending, hydrothermally-altered fault zone near an area of massive rhyolites that Drewes (1979) believes may be the site of a caldera of Cretaceous age (locality D in Fig. 11). The analogy to the situation in the Sierrita Mountains is quite apparent. The area of massive rhyolites certainly warrants a geophysical investigation in order to determine if a mineralized intrusive lies buried at depth.

CONCLUSIONS

This study has demonstrated that multivariate analysis of computer-registered data sets is an effective means for rapidly targeting areas of mineralization potential. Although the exploration model employed in this study was designed for the direct detection of near-surface porphyry copper deposits of large areal extent, the method succeeded in detecting both large and small features that may indirectly lead to the discovery of nearby unknown deposits. These results indicate that the design of the future porphyry copper exploration models should be oriented more towards detecting the indirect indicators of mineralization, such as hydrothermally-altered fault zones and anomalously radioactive pediment slopes, rather than the deposit

itself. Using the data types employed in this study as an example, the variables K, U, K/Th, U/Th and aeromagnetism would serve best when exploring for hydrothermally-altered fault zones while the variables K, K/Th, MSS 5/MSS 4, and MSS 6/MSS 7 would probably be more important when searching the pediment slopes below eroding mountain fronts. Additional data types would of course improve the detection capability of the method.

ACKNOWLEDGEMENTS

We wish to extend special thanks to Ed Keh, Chuck Smith, Tim Grogan, and Marijan Poljak for their invaluable contributions during the course of this study. We also wish to thank the National Science Foundation for their support through Grant No. ENG-7820466.

REFERENCES

- Anuta, P.E., 1977, Computer-Assisted Analysis Techniques for Remote Sensing Data Interpretation, *Geophysics*, Vol. 42(3), pp. 468-481.
- Arizona Bureau of Mines, 1969, Geologic map of Arizona.
- Brown, A.S. and Cathro, R.J., 1976, A Perspective of Porphyry Deposits in Porphyry Deposits of the Canadian Cordillera, CIM Special Volume No. 15, pp. 7-16.
- Cooper, J.R., 1973, Geologic map of the Twin Buttes quadrangle, southwest of Tucson, Pima County, Arizona, U.S. Geol. Survey Misc. Geol. Inv. Map I-745.
- Davis, J.D. and Guilbert, J.M., 1973, Distribution of the Radioelements Potassium, Uranium, and Thorium in Selected Porphyry Copper Deposits, *Econ. Geology*, Vol. 68(2), pp. 145-160.
- Drewes, H., 1979, Preliminary Tectonic Map of Southeast Arizona, U.S.G.S. Open-File Rept. 79-775.
- Hunt, G.R. and Ashley, R.P., 1979, Spectra of Altered Rocks in the Visible and Near Infrared, *Econ. Geol.*, Vol. 74(7), pp. 1613-1629.
- Kowalik, W.S., Burgess, L.A., and Lyon, R.J.P., 1980, Reconnaissance Exploration for Limonitic Outcrops in Parts of Churchill and Mineral Counties, Nevada Using Landsat Digital Data, Stanford Remote Sensing Laboratory Tech. Rept. 80-3, Stanford University, 36 p.

- Lootens, D.J., 1966, Geology and Structural Environment of the Sierrita Mountains, Pima County, Arizona in Ariz. Geol. Soc. Digest, Vol. 8, pp. 33-56.
- Lowell, J.D. and Guilbert, J.M., 1970, Lateral and Vertical Alteration -- Mineralization Zoning in Porphyry Ore Deposits, Econ. Geology, Vol. 65, pp. 373-408.
- Lynch, D.W., 1966, The Economic Geology of the Esperanza Mine and Vicinity in Geology of the Porphyry Copper Deposits of Southwestern North America, ed. by S.R. Titley and C.L. Hicks, Univ. of Ariz. Press, pp. 267-279.
- Lyon, R.J.P., 1977, Mineral Exploration Applications of Digitally Processed Landsat Imagery in Proc. of the First William T. Pecora Memorial Symp., Oct. 1975, Sioux Falls, SD, U.S.G.S. Prof. Paper 1015, pp. 271-292.
- Moolick, R.T. and Durek, J.J., 1966, The Morenci District in Geology of the Porphyry Copper Deposits of Southwestern North America, ed. by S.R. Titley and C.L. Hicks, Univ. of Ariz. Press, pp. 221-231.
- Moxham, R.M., Foote, R.S., and Bunker, C.M., 1965, Gamma-Ray Spectrometer Studies of Hydrothermally Altered Rocks, Econ. Geology, Vol. 60, pp. 653-671.
- Salmon, B. and Vincent, R.K., 1974, Surface Compositional Mapping in the Wind River Range and Basin, Wyoming by Multi-spectral Techniques Applied to ERTS-1 Data in Proc. Ninth Int. Symp. on Remote Sensing of the Environment, Environmental Research Institute of Michigan, Ann Arbor, pp. 2005-2012.

- Schwartz, G.M., 1966, The Nature of Primary and Secondary Mineralization in Porphyry Copper Deposits in Geology of the Porphyry Copper Deposits of Southwestern North America, ed. by S.R. Titley and C.L. Hicks, Univ. of Ariz. Press, pp. 41-50.
- Simpson, C.J., 1978, Landsat: Developing Techniques and Applications in Mineral and Petroleum Exploration, BMR Journal of Australian Geology and Geophysics, Vol. 3, pp. 181-191.
- U.S. Bureau of Mines, 1977, Mining and Mineral Operations in the Rocky Mountain States, 87 p.
- Vincent, R.K., 1973, Spectral Ratio Imaging Methods for Geological Remote Sensing From Aircraft and Satellites in Management and Utilization of Remote Sensing Data, a Symposium of the American Society of Photogrammetry, Sioux Falls, SD, pp. 377-397.